International Journal of Engineering & Technology, 7 (1.1) (2018) 184-188

International Journal of Engineering & Technology

Website: www.sciencepubco.com/index.php/IJET

Research paper

Performance comparisons of particle swarm optimization, echo state neural network and genetic algorithm for vegetation segmentation

Rincy Merlin Mathew [1*], S. Purushothaman [2], P. Rajeswari [3]

[1] *Research Scholar, Department of Computer Science and Engineering, VELS University, Chennai, India*
[2] *Chennai, India*
[3] *Department of Computer Science, Girls Community College, King Khalid University, Abha, Saudi Arabia*
**Corresponding author E-mail:Mathew.rincymerlin@gmail.com*

Abstract

This article presents the implementation of vegetation segmentation by using soft computing methods: particle swarm optimization (PSO), echostate neural network(ESNN) and genetic algorithm (GA). Multispectral image with the required band from Landsat 8 (5, 4, 3) and Landsat 7 (4, 3, 2) are used. In this paper, images from ERDAS format acquired by Landsat 7 'Paris.lan' (band 4, band 3, Band 2) and image acquired from Landsat 8 (band5, band 4, band 3) are used. The soft computing algorithms are used to segment the plane-1(Near infra-red spectra) and plane 2(RED spectra). The monochrome of the two segmented images is compared to present performance comparisons of the implemented algorithms.

Keywords: *Particle Swarm Optimization, Echostate Neural Network, Genetic Algorithm, Vegetation Segmentation.*

1. Introduction

This paper presents identifications of vegetation in a remote sensed image. The main purpose is to make a continuous monitoring the growth of vegetation. The beneficiaries are government, owners of the vegetation. The government can benefit about the total quantity of vegetation in an area. In this work, particle swarm optimization, echostate neural network and genetic algorithm are used for segmentation and identifying the vegetation area.

Masroor et al.,[1], discussed about the traditionally pixel-based and statistics-oriented change detection techniques which focus mainly on the spectral values and ignore the spatial context. A review of object-based change detection techniques is compassed. In addition, a study on the spatial data mining techniques in image processing and change detection from remote sensing data is discussed. The significance of the rapid change in the image data volume and multiple sensors and related confrontations on the growth of change detection techniques are highlighted.

Hannes et al.,[2], introduced the importance of annual deforestation information for understanding and alleviating deforestation. An image compositing approach is used to transform 2224 Landsat images in a spatially continuous and cloud free environment. In addition, a random forest classifier is used to derive annual deforestation patterns.

Pasher et al.,[3], introduced methods for earth observation that can be used to enumerate and keeps track of LWF (linear woody features) across the environment. In the meanwhile individual structure can be manually systemized and is concentrated on the enhancement of methods using line intersect sampling (LIS) for estimating LWF as an indicator of environmental assessment in agricultural topography. This approach is used mainly for large regions where environmental assessment is profoundly concerned in agricultural topography which is manipulated.

Curtis et al.,[4], evaluated the significance of topographic correction on trend-based forest change detection conclusions by analyzing the location and an aggregation of changes is classified on an image synthesis with and without a topographic correction. A large amount of change in area is identified when no topographic rectification is correlated to the synthesized image.

Zhao-Liang et al.,[5], reviewed the present significance of certain remote sensing algorithms for estimating LST from thermal infrared (TIR) data. A survey on algorithms to gain LST from space-based TIR measurements is accomplished based on the speculated circumstances. In addition, an emphasis on TIR data obtained from polar-orbiting satellites is done due to the extensive use, comprehensive relevance and higher spatial resolution in contradiction to geostationary satellites.

O'Loughlin et al.,[6], developed the first global 'Bare-Earth' Digital Elevation Model (DEM) based on the Shuttle Radar Topography Mission (SRTM) for all landmasses between 60N and 54S. The result of 'Bare-Earth' SRTM product shown global improvements greater than 10min the bias over the original SRTM DEM in vegetated areas compared with ground elevations determined from ICESat data with a significant reduction in the root mean square error from over 14 m to 6 m globally.

Andrew et al.,[7], introduced methods by using a small, unpiloted aerial system to acquire aerial photographs and processing these using structure-from-motion photogrammetry, three-dimensional models were generated depicting the vegetation structure of semi-arid ecosystems at seven sites across a grass–to shrub transition zone. The result is concerned about the how products from inexpensive UAS coupled with structure- from- motion photogrammetry can produce ultra-fine grain biophysical data products, which has the capability to alter precise knowledge of

ecology in ecosystems with either spatially or temporally unorganized canopy cover.

Min Feng et al.,[8], estimated a mechanism based on per-pixel estimates of percentage tree cover and their associated uncertainty, the dataset currently signifies binary forest cover in nominal 1990, 2000, and 2005 epochs, besides gains and losses due to time.

Mihretab et al.,[9], introduced methods for the supervised classification technique to classify and analyze the total forest-cover change in Eritrea. The study concluded that deforestation is one of the leading causes of environmental degradation in the country and it might be caused by human factors as well as due to climate change, i.e., by prolonged drought and inadequate and erratic rainfall.

Mohamed et al., [10] developed a GIS based approach for land use suitability assessment which will assist land managers and land use planners to identify areas with physical constraints for a range of nominated land uses. Also, GIS has been used to compare the appropriate method for main crops based on the needs of the crops and the quality and properties of land. Suitability and capability maps for each land use were established to exemplify an appropriate method to display the spatial representation of soils suitable for agriculture.

Yu Zhang et al., [11], analysed a study on the configurations and spatial-temporal processes of landscape. Redundancy analysis (RDA) and variation partitioning were performed to identify the main driving forces and to quantify the unique, shared, and total explained variation of the sets of variables. The results of the variation partitioning indicated complex interrelationships among all of the pairs of driver sets.

Adrien Michez et al., [12], proposed a technique for an easily reproducible approaches framework using Unmanned Aerial Systems (UAS) imagery. Supervised classification based on the random forests algorithm was used to ascertain the most appropriate variable derived from UAS imagery for mapping invasive plant species.

Gayantha et al., [13], developed a mechanism concerned an extraction of spectrally pure pixels of the area using Pixel Purity Index (PPI), identification of the selected end member spectrum using the Modified Gaussian Method(MGM) and mapping of logically identified end members using the Spectral Angle Mapper (SAM) method. Mapping results determine both the capabilities and the limitations of the MGM method of convolution and the SAM method of spectral matching as efficient tools for compositional representation of morphological appearance on the lunar surface.

Inka et al., [14], examined the classification of forest land using airborne laser scanning (ALS) data, satellite images and sample plots of the Finnish National Forest Inventory (NFI) as training data and identified best performing metrics for classifying forest land attributes.

Trung et al., [15], introduced method for Landsat data at high spatial resolution with 8-day MODIS data to produce high spatial and temporal resolution image time-series. The method namely Spatial Temporal Adaptive Algorithm for mapping Reflectance Change (STAARCH) fusion method was introduced to successfully produce a time-series of disturbances with high overall accuracy (89–92%) in mixed forests in southeast Oklahoma. By the use of high spatial and temporal resolution imagery datasets, they recognized the economic and environmental factors, as well as the consequences of those changes in a better way.

Robinson et al., [16], tested the capable of WV2 imagery that provided desirable portability capable for detecting other species where spectral/spatial resolution or coverage. New generation satellite sensors are removing barriers from previously preventing widespread adoption of remote sensing technologies in natural resource management.

2. Methodology: implementation of the algorithms for vegetation image segmentation

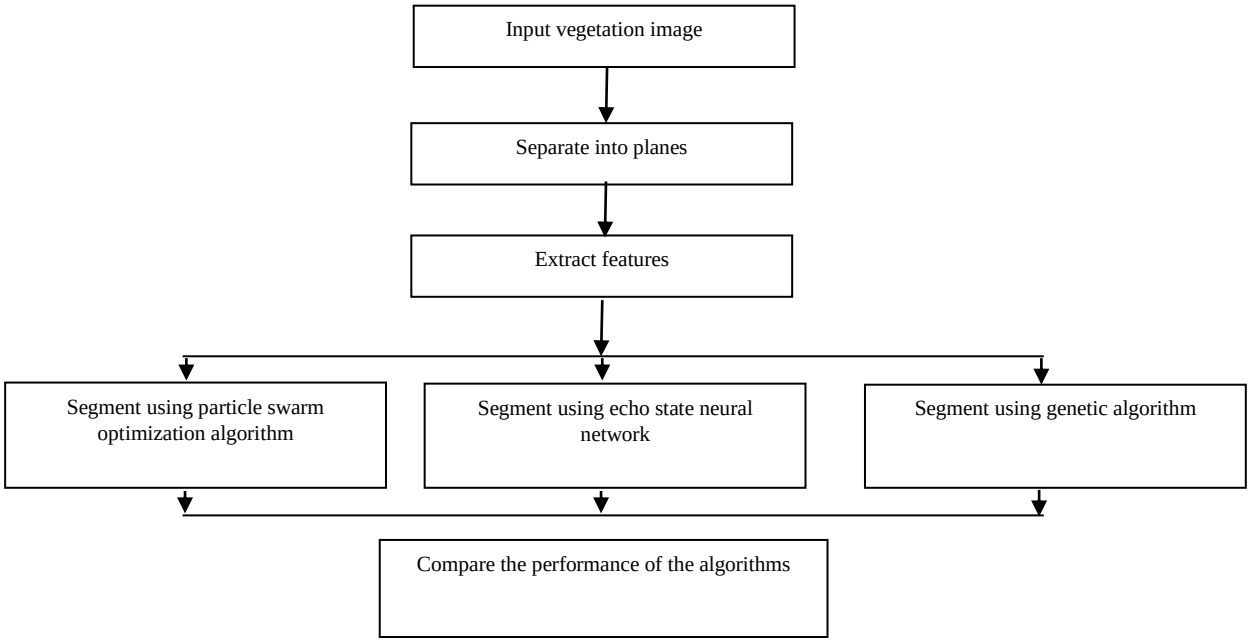

Fig. 1: Schematic flow for vegetation image segmentation

Figure 1 presents a schematic flow of the research work. Landsat image is separated into three plane. Each plane is segmented by using the particle swarm optimization algorithm, echo state neural network and genetic algorithm. The performances of the three algorithms are compared.

Data collection

A sample database has been presented directly taken from the database of the Matlab R2013. LANDSAT Thematic Mapper image covering part of Paris, France, made available courtesy of Space Imaging, LLC with seven spectral bands are stored in one file in the Erdas LAN format. The LAN file, contains a 7-band 512-by-512 Landsat image. This file is band interleaved by line (BIL) in order of increasing band number.

Thematic Mapper 4, 3, and 2 bands cover the near infrared (NIR), the visible red, and the visible green parts of the electromagnetic spectrum. When they are mapped to the red, green, and blue planes, respectively, of an RGB image the result is a standard color-infrared (CIR) composite.

Statistical feature extraction

The features are obtained from moving 3x3 overlapping windows in an image using the following equations:

$V1=1/d \sum$ (intensity values) (1)
Where d = Samples in a frame and
V1 = Mean value of intensity values
$V2=1/d \sum$ (intensity values –V1)) (2)
Where V2=Standard Deviation of intensity values
V3=maximum (intensity values) (3)
V4=minimum (intensity values) (4)
$V5=\text{norm (intensity values)}^2$ (5)
Where V5 = Energy value of frequency

The implementing of the feature extraction is given as follows

Step 1: Read a landsat image and split into 3X3 windows.
Step 2: Calculate the statistical features.
Step 3: Find the mid_pixel value of the Pattern C_{center_pixel}.
Step 4: Find the number of values greater than the Median Values, U_m.
Step 5: Calculate segment_value using $C_{center\_pixel} + (1/Tcc) * (U_m – (bs/2))$.
A combination is created of three individual monochrome images, in which each is assigned a given color; this is defined **color composite** and is useful for photo interpretation (NASA, 2013). Color composites are usually expressed as:

"R G B = Br Bg Bb" (6)

where:

1) R stands for Red;
2) G stands for Green;
3) B stands for Blue;
4) Br is the band number associated to the Red color;
5) Bg is the band number associated to the Green color;
6) Bb is the band number associated to the Blue color.

The Figure 2 Color composite of a Landsat 8 image shows a color composite "R G B = 4 3 2" of a Landsat 8 image (for Landsat 7 the same color composite is R G B = 3 2 1) and a color composite "R G B = 5 4 3" (for Landsat 7 the same color composite is R G B = 4 3 2). The composite "R G B = 5 4 3" is useful for the interpretation of the image because vegetation pixels appear red (healthy vegetation reflects a large part of the incident light in the near-infrared wavelength, resulting in higher reflectance values for band 5, thus higher values for the associated color red).

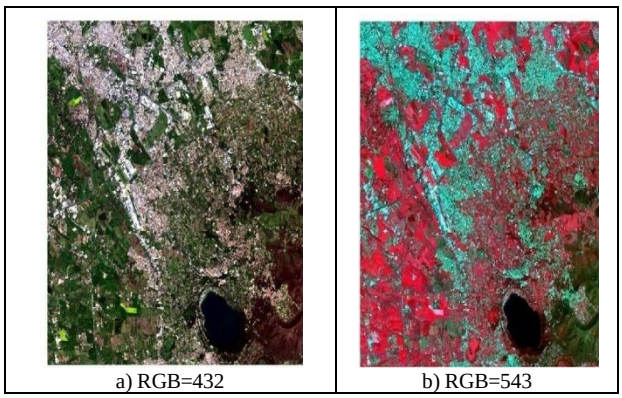

a) RGB=432 b) RGB=543

Fig. 2: Original RGB image with different bands

Figure 3 presents original image and the segmented image of plane-1. Most of the information is thickly segmented. Figure 4 presents original image and the segmented image of plane-2. Segmentation in plane-2 presents acceptable results. Figure 5 presents original image and the segmented image of plane-3. Segmentation in this plane is almost similar to the segmented results obtained from plane-2.

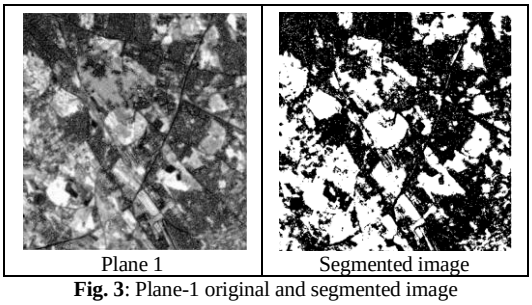

Plane 1 Segmented image

Fig. 3: Plane-1 original and segmented image

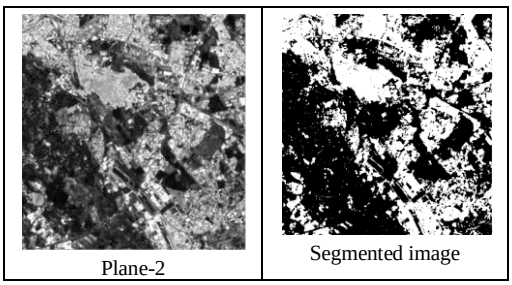

Plane-2 Segmented image

Fig. 4: Plane-2 Original and segmented image

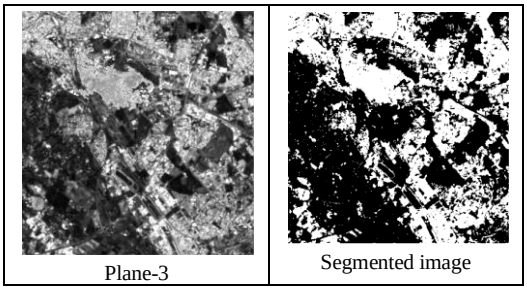

Plane-3 Segmented image

Fig. 5: Plane-3 original and segmented image

Particle swarm optimization

Birds searching for food is described by the particle swarm optimization algorithm. They try to locate food at far away distance. A bird is called particle. Fitness values are evaluated by using fitness function to find out if the birds have reached their food. The birds move with specific velocities and directions to reach the food.
The concept of generations is used for searching the location of food. Two best values are used in each generation. Present best value and global best value.
After finding the two best values, the particle updates its velocity and positions with following equation (7) and (8).

vel[] = vel[] + Fc1 * rand() * (presentbest[] - present[]) + c2 * rand() * (globalbest[] - present[]) (7)
present[] = present[] + v[] (8)
vel[] is the particle velocity,
present[] is the current particle (solution).
presentbest[] and globalbest[] are defined as stated before.
rand () is a random number between (0,1).
Fc1, Fc2 are learning factors.

PSO parameter control

The number of particles: It can be anything of our choice according to the problem. It can be up to 1000 as well.

Vmax: It indicates velocity changes. Vmax can be any value split into a range from negative to positive.
Learning factors: Fc1 and Fc2 usually can be any value greater than 0.
The stop condition: the maximum number of iterations the PSO execute and the minimum error requirement.

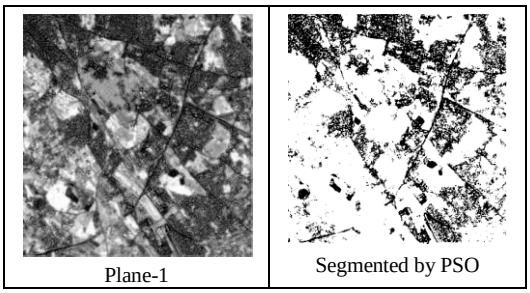

Fig. 6: Segmentation of plane-1 by PSO

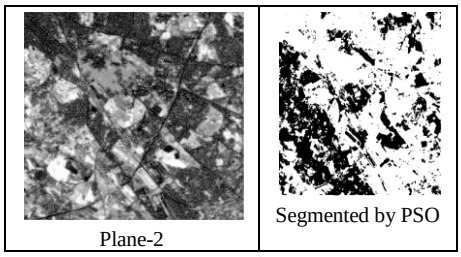

Fig. 7: Segmentation of plane-2 by PSO

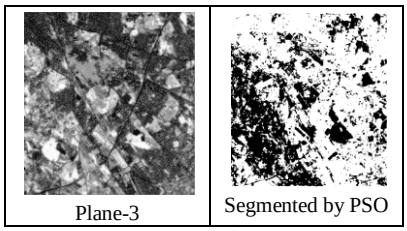

Fig. 8: Segmentation of plane-3 by PSO

Figures 6-8 present the segmentation of three planes of vegetation images by PSO.

Echo state neural network

An Artificial Neural Network (ANN) is an abstract stimulation of a real nervous system that contains a collection of neuron units, communicating with each other via axon connections. Artificial neural networks are computing elements which are based on the structure and function of the biological neurons. These networks have nodes or neurons which are described by difference or differential equations.

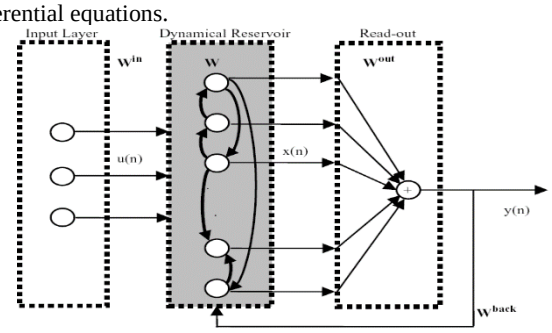

Fig. 9: An echo state network (ESNN)

The echo state condition is defined in terms of the spectral radius (the largest among the absolute values of the eigenvalues of a matrix, denoted by (|| ||) of the reservoir's weight matrix (|| W ||<1). This condition states that the dynamics of the ESNN is uniquely controlled by the input, and the effect of the initial states vanishes. The current design of ESNN parameters relies on the selection of spectral radius. There are many possible weight matrices with the same spectral radius, and unfortunately they do not perform at the same level of mean square error (MSE) for functional approximation.
The recurrent network is a reservoir of highly interconnected dynamical components, states of which are called echo states. The memory less linear readout is trained to produce the output.
The ESNN neural network given in Figure 9 with M input units, N internal PEs, and L output units. The value of the input unit at time n is $u(n) = [u_1(n), u_2(n), \ldots, u_M(n)]^T$, The internal units are $x(n) = [x_1(n), x_2(n), \ldots, x_N(n)]^T$, and Output units are $y(n) = [y_1(n), y_2(n), \ldots, y_L(n)]^T$. The connection weights are given

a) in an (NxM) weight matrix $W^{back} = W_{ij}^{back}$ for connections between the input and the internal PEs,
b) in an N×N matrix $W^{in} = W_{ij}^{in}$ for connections between the internal PEs
c) in an L×N matrix $W^{out} = W_{ij}^{out}$ for connections from PEs to the output units and
d) in an N×L matrix $W^{back} = W_{ij}^{back}$ for the connections that project back from the output to the internal PEs.

The activation of the internal PEs (echo state) is updated according to

$$x(n+1) = f(W^{in}u(n+1) + Wx(n) + W^{back}y(n)), \quad (9)$$

where $f = (f_1, f_2, \ldots, f_N)$ are the internal PEs' activation functions. Here, all f_i's are hyperbolic tangent functions $\frac{e^x - e^{-x}}{e^x + e^{-x}}$.
The output from the readout network is computed according to

$$y(n+1) = f^{out}(W^{out}x(n+1)), \quad (10)$$

where $f^{out} = (f_1^{out}, f_2^{out}, \ldots, f_L^{out})$ are the output unit's nonlinear functions. Generally, the readout is linear so f^{out} is identity.

Genetic algorithm for segmentation

Genetic Algorithms are search algorithms for optimization based on mechanics of natural selection and genetics. The power of these algorithms is derived from a very simple heuristic assumption that the best solution will be found in the regions of solution space containing high proposition if good solution and these regions can be identified by judicious and robust sampling of the solution space. The computations are carried out in the stages to get results in one (or) more generation or iteration. The three stages are:

1) Reproduction
2) Cross-over
3) Mutation

Characteristics of genetic algorithm

1) Genetic algorithms manipulate decision or control variable representations at a string level to exploit similarities among high-performance strings.
2) GAs deal with parameters of finite length, which are coded using a finite alphabet.
3) GAs can deal effectively with a broader class of functions than can many other procedures.
4) Evaluation of the performance of candidate solutions is found using objective, payoff information.
5) GAs find safety in numbers, by maintaining a population of well-adapted sample points, the probability of reaching a false peak is reduced.
6) The search starts from a population of many points, rather than starting from just one point.
7) GAs achieve much of their breadth by ignoring information except that concerning payoff. GAs remain general by exploiting information available in any search problem. GAs process similarities in the underlying coding together with information ranking the structures according to their survival capability in the current environment. By exploiting such widely-

available information, GAs may be applied to virtually any problem.

Fitness function

A fitness function is formulated to segment the image. It is expressed as follows:

Segment= a1xb1 +a2xb2+a3xb3 +a4xb4 +a5xb5+a6xb6+ a7xb7+ a8xb8+a9xb9 (11)

Generations or iterations

Formulations of new sets of chromosomes is called generations. New generation of chromosomes is obtained by, pairing of chromosomes, splitting chromosomes, crossing the chromosome pairs, and mutating the bits of the chromosomes.

Cross Over: Cross over is a recombinant operates that taken two individuals and cuts theirs chromosome strings at some randomly-chosen position. The purpose of crossover is searching the parameter space and the search needs to the performed such that the information stored in the parent strings are maximally preserved because these parent strings are instances of good strings selected using the reproduction operator. For each string in the mating pool, random numbers between 0 and 1 are generated. The strings with random numbers less than the crossover probabilities are selected for crossover operation. Cross sites are randomly generated for randomly selected pairs thou the section of strings after the cross sites are just swapped between two adjacently selected strings after cross over the population is worked out. Generally the cross over are classified as

1. Single point cross over (L=1)
2. Multipoint cross over (L=2,3….)

Mutation: In the mutation operation, random numbers between 0 and 1 are generated for each solution. The string with random numbers less than the mutation operation. Since mutation takes place within a string, two mutation points are randomly generated for each selected strings. The genes corresponding to the mutation points are just swapped after mutation the population is worked out.

String Length: The string lengths are taken as 40 in each chromosome for splitting it. The strings representing the individuals in the initial population are randomly generated. These binary strings are decoded. For further evaluation. The population for the next generation is created depending upon the evaluation results of the first generation and the GA parameters. Generation of the population for subsequent generation depends on the selection operator as well as on the crossing cover and mutation probability. The algorithm repeats the same process by generating the new population and evaluating its fitness.

3. Conclusion

The work has used landsat vegetation database acquired from the internet resource. Soft algorithms are used for segmenting the vegetation images.

1. The particle swarm optimization algorithm(PSO) is used for the segmentation of the image. The performance of the PSO depends on the number of particles, and the velocity of the articles. The number of gray levels in the image influences the segmentation performance of the PSO. The computational complexity of the PSO is much more, however its performance in segmenting the image best among the three implemented algorithms.
2. The echostate neural network performance depends on the initial weights allotted to the interconnection matrix, the number of reservoirs present in the hidden layer. The performance of the algorithm is equally better and similar to the performance of the PSO.
3. The performance of the genetic algorithm involves generation of binary random numbers, cross over length, mutation sequence and the objective function used. The algorithms requires many generations before it reaches the specified target values. The performance of the algorithm is good when compared to the other two algorithms. However, it requires intuitive random generators for population and deciding the correct cross overlength for the mutation process.

References

[1] Hussain M, Chen D, Cheng A, Wei H & Stanley D, "Change detection from remotely sensed images: From pixel-based to object-based approaches", *ISPRS Journal of Photogrammetry and Remote Sensing*, Vol.80, (2013), pp.91–106.

[2] Müller H, Griffiths P & Hostert P, "Long-term deforestation dynamics in the Brazilian Amazon-Uncovering historic frontier development along the Cuiabá–Santarém highway", *International Journal of Applied Earth Observation and Geoinformation*, Vol.44, (2016), pp.61–69.

[3] Pasher J, McGovern M & Putinski V, "Measuring and monitoring linear woody features in agricultural landscapes through earth observation data as an indicator of habitat availability", *International Journal of Applied Earth Observation and Geoinformation*, Vol.44, (2016), pp.113–123.

[4] Chance CM, Hermosilla T, Coops NC, Wulder MA & White JC, "Effect of topographic correction on forest change detection using spectral trend analysis of Landsat pixel-based composites", *International Journal of Applied Earth Observation and Geoinformation*, Vol.44, (2016), pp.186–194.

[5] Li ZL, Tang BH, Wu H, Ren H, Yan G, Wan Z, Trigo IF & Sobrino JA, "Satellite-derived land surface temperature: Current status and perspectives", *Remote Sensing of Environment*, Vol.131, (2013), pp.14–37.

[6] O'Loughlin FE, Paiva RCD, Durand M, Alsdorf DE & Bates PD, "A multi-sensor approach towards a global vegetation corrected SRTM DEM product", *Remote Sensing of Environment*, Vol.182, (2016), pp.49–59.

[7] Cunliffe AM, Brazier RE & Anderson K, "Ultra-fine grain landscape-scale quantification of dryland vegetation structure with drone-acquired structure-from-motion photogrammetry", *Remote Sensing of Environment*, Vol.183, (2016), pp.129–143.

[8] Feng M, Sexton JO, Huang C, Anand A, Channan S, Song XP, Song DX, Kim DH, Noojipady P & Townshend JR, "Earth science data records of global forest cover and change: Assessment of accuracy in 1990, 2000, and 2005 epochs", *Remote Sensing of Environment*, Vol.184, (2016), pp.73-85.

[9] Ghebrezgabher MG, Yang T, Yang X, Wang X & Khan M, "Extracting and analyzing forest and woodland cover change in Eritrea based on landsat data using supervised classification", *The Egyptian Journal of Remote Sensing and Space Sciences*, Vol.19, (2016), pp. 37–47.

[10] AbdelRahman MAE, Natarajan A & Hegde R, "Assessment of land suitability and capability by integrating remote sensing and GIS for agriculture in Chamarajanagar district, Karnataka, India", *The Egyptian Journal of Remote Sensing and Space Sciences*, Vol.19, (2016), pp.125–141.

[11] Zhang Y, Wang T, Cai C, Li C, Liu Y, Bao Y & Guan W," Landscape pattern and transition under natural and anthropogenic disturbance in an arid region of north western China", *International Journal of Applied Earth Observation and Geoinformation*, Vol.44, (2016), pp.1–10.

[12] Michez A, Piégay H, Jonathan L, Claessens H & Lejeune P, "Mapping of riparian invasive species with supervised classification of Unmanned Aerial System (UAS) imagery", *International Journal of Applied Earth Observation and Geoinformation*, Vol.44, (2016), pp.88–94.

[13] Kodikara GR, Chauhan P & Chatterjee RS, "Spectral mapping of morphological features on the moon with MGM and SAM", *International Journal of Applied Earth Observation and Geoinformation*, Vol.44, (2016), pp.31-41.

[14] Pippuri I, Suvanto A, Maltamo M, Korhonen KT, Pitkänen J & Packalen P, "Classification of forest land attributes using multi-source remotely sensed data", *International Journal of Applied Earth Observation and Geoinformation*, Vol.44, (2016), pp.11–22.

[15] Tran TV, de Beurs KM & Julian JP, "Monitoring forest disturbances in southeast oklahoma using landsat and MODIS images", *International Journal of Applied Earth Observation and Geoinformation*,Vol.44, (2016), pp.42–52.

[16] Robinson TP, Wardell-Johnson GW, Pracilio G, Brown C, Corner R & van Klinken RD, "Testing the discrimination and detection limits of World View-imagery on a challenging invasive plant target", *International Journal of Applied Earth Observation and Geoinformation*, Vol.44, (2016), pp.23–30.